ION REPULSION WITHIN MEMBRANES

R.Y. TSIEN
Dept. of Physiology-Anatomy, University of California, Berkeley, California 94720
S.B. HLADKY
Department of Pharmacology, University of Cambridge, Cambridge CB2 2QD, England

ABSTRACT The adsorption of hydrophobic ions such as tetraphenylborate to thin lipid membranes is known to saturate at ~0.1 ion/(nm)^2. This saturation can be quantitatively explained by electrostatic repulsion between the ions if they are treated as discrete, mobile particles that adsorb within the lipid at least partially removed from the aqueous phases. The electrochemical potential of the ions as a function of their surface density can be expressed as a virial expansion, which in principle exactly describes the equilibrium properties of the physical model. The first few terms of the virial expansion are calculated and an approximation is considered for higher-order terms. The model has only two adjustable parameters, the depth of the adsorption sites into the lipid and the adsorption constant in the absence of repulsion. The mobile, discrete charge model can give much better fits to the equilibrium data for tetraphenylborate adsorbed at up to 0.1 ion/(nm)^2 to membranes and monolayers (Andersen et al., 1978) than those obtainable from either the smeared charge or hexagonal lattice models.

THE VIRIAL EXPANSION FOR THE ELECTROCHEMICAL POTENTIAL OF ADSORBED IONS

The mutual electrostatic repulsion of hydrophobic ions adsorbed to a single lipid-aqueous interface has already been calculated using a simple physical model and the technique of virial expansions (Tsien, 1978). In this model the ions are treated as mobile discrete charges adsorbed within a homogeneous lipid layer at a fixed distance l from the interface with aqueous saline. Cylindrical coordinates r, θ, z were established with the interface as the plane $z = 0$. At the ion densities of interest, up to ~1 ion/10 (nm)^2, typical ion separations are much greater than the Debye length in the saline, 0.3 nm in 1 M NaCl. Therefore the aqueous phases are treated as perfect conductors.[1] For detailed justification of this approximation see Tsien, 1978. The potential energy for the repulsion of any pair of ions is then

$$q\varphi_m(r) = \frac{q^2}{4\pi\epsilon\epsilon_0}\left(\frac{1}{r} - \frac{1}{\sqrt{r^2 + 4l^2}}\right) \simeq \frac{q^2}{4\pi\epsilon\epsilon_0} \cdot \frac{2l^2}{r^3} \quad (1)$$

where q is the charge on each ion, ϵ is the relative dielectric constant of the lipid, ϵ_0 is the permittivity of free space, and r is the lateral separation of the ions.

For a bilayer membrane of thickness d there is now a second interface at $z = d$ and a second adsorption layer at $z = d - l$. The potential energy of interaction for a pair of ions, one of which is at cylindrical coordinates $(0, 0, l)$ and the other at (r, θ, z), is (Barlow and MacDonald, 1967):

$$q\varphi(r, z) = \frac{q^2}{\pi\epsilon\epsilon_0 d}\sum_{k=1}^{\infty} \sin\left(\frac{k\pi l}{d}\right)\sin\left(\frac{k\pi z}{d}\right)K_0\left(\frac{k\pi r}{d}\right), \quad (2)$$

regardless of θ. K_0 is a modified Bessel function. For large $(k\pi r/d)$, K_0 decays approximately as $(d/2kr)^{1/2}\exp(-k\pi r/d)$, so that the series in Eq. 2 converges very rapidly. For $r > d$ the potential falls off quite sharply.

To help the reader get a feeling for the electrostatic pair potentials in a monolayer and bilayer (Eqs. 1 and 2, respectively), Fig. 1 *a* presents such potential energies as a function of lateral separation r. For the equilibrium properties of the bilayer, Eq. 2 is to be evaluated for two conditions: when the two ions are in the same adsorption layer, i.e., both at $z = l$ or both at $z = d - l$, or when the two ions are on opposite sides of the membrane, one at $z = l$, the other at $z = d - l$.

The crucial next step is to translate Eq. 2, which gives the electrostatic repulsion of just two ions at assumed

[1]It is easy to relax partly this assumption that the aqueous phases have sufficient salt to act like perfect conductors. Thus the lipid-aqueous interface can be taken to be an isopotential surface whose electrostatic potential and local concentration of tetraphenylborate with respect to the bulk aqueous phases are given by the standard Gouy-Chapman formulae. Much evidence has accumulated (McLaughlin, 1977) that a smeared-charge Gouy-Chapman treatment is surprisingly accurate for the effects of electrostatic fields in the aqueous phase, even if smeared charges are inadequate to treat the much stronger effects of fields in the lipid phase. Small correction terms have to be added to equations 3, 8, 9, 12, and 14. Because the maximum Gouy-Chapman potential is < 10 mV at charge densities of interest (up to 2 μC/cm^2) and 1 M ionic strength, the appearance of Figs. 2–5 is hardly altered, so for simplicity the Gouy-Chapman correction has been left out.

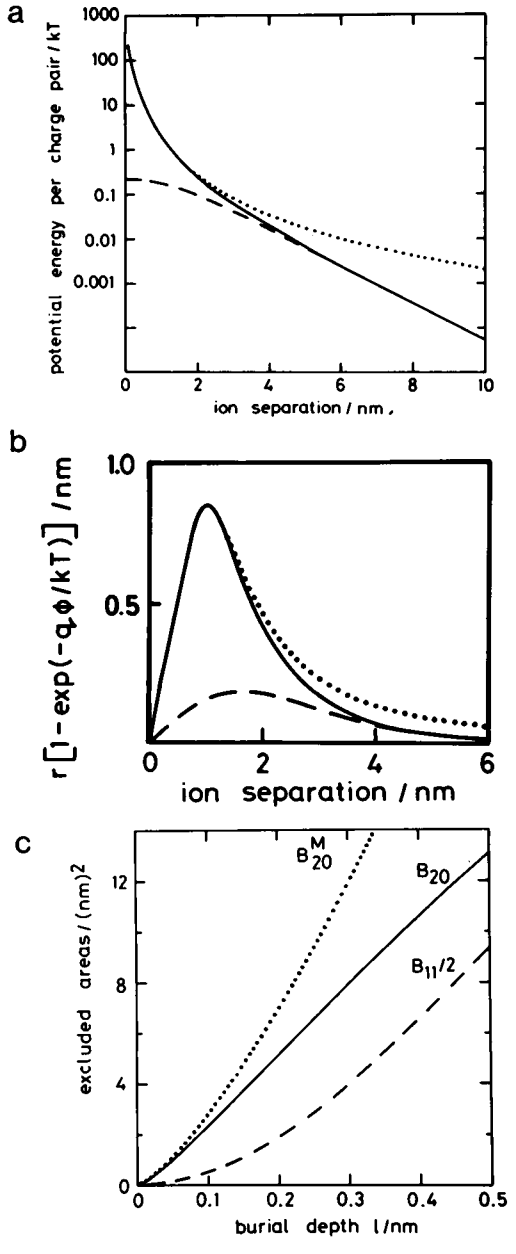

FIGURE 1 (*a*) The potential energy of interaction (normalized to kT at: 295°K) of a pair of ions: ——, both adsorbed to the same side of the membrane, $q\varphi(r, l)$; – – – –, one adsorbed on each side, $q\varphi(r, d - l)$; · · · ·, both adsorbed in a monolayer, $q\varphi_{im}(r)$. The curves have been calculated using $\epsilon = 2.1$, $l = 0.20$ nm, and $d = 3.51$ nm. This value of d is calculated from ϵ and the observed membrane capacity of 0.53 μF/cm^2 (Andersen et al., 1978). The abscissa r is the projection onto one interface of the separation of the ions. For $r \ll d$, the other interface has little effect, so that the solid and dotted lines converge. Similarly for $r \gg d$, an ion on either surface looks the same, so the solid and dashed lines converge, but the presence of two surfaces rather than one greatly attenuates the interaction. (*b*) The integrands of the configuration integrals for B_{20}, ——, $\frac{1}{2}B_{11}$, – – – –, and B_{20}^m, · · · ·, based on the pair potential energies above. (*c*) The second virial coefficients B_{20}, B_{11} and B_{20}^m as functions of the depth of burial l. For B_{20} and B_{20}^m the values may be interpreted as the area excluded to one ion by the presence of another on the same side of the bilayer, B_{20}, or on a monolayer, B_{20}^m. For ions on opposite sides of the membrane the excluded area is $\frac{1}{2}B_{11}$ and it is $\frac{1}{2}B_{11}$ which is plotted. Over the entire range of B_{20}^m shown, B_{20}^m differs from $B_{20} + \frac{1}{2}B_{11}$ by less than the line width; for $l = 0.5$ nm, B_{20}^m is larger by 5%.

positions in the membrane, into thermodynamic functions for an ensemble of $>10^{11}$ ions whose positions are fluctuating unknowns. This step is easily accomplished by a virial expansion technique (Hill, 1960) with the slight complication that the ions on each side of the membrane must be counted separately, because the number on each side may be different and because repulsions from across the membrane are different from same-side repulsions. Thus the electrochemical potential of the ions in the adsorption layer $z = l$ is

$$\mu' = \mu^0 + kT \ln n' + ql\Delta V/d + 2B_{20}n'kT + B_{11}n''kT + \tfrac{3}{2}B_{30}n'^2kT + B_{21}n'n''kT + \tfrac{1}{2}B_{21}n''^2kT + \cdots \quad (3a)$$

while for the ions at $z = d - l$,

$$\mu'' = \mu^0 + kT \ln n'' + q(d - l)\Delta V/d + 2B_{20}n''kT + B_{11}n'kT + \tfrac{3}{2}B_{30}n''^2kT + B_{21}n'n''kT + \tfrac{1}{2}B_{21}n'^2kT + \cdots . \quad (3b)$$

In Eq. 3a and b, μ^0 is the electrochemical potential in a hypothetical reference state with no repulsions and $n' = 1$, ΔV is the externally applied electric potential at $z = d$ relative to that at $z = 0$, n' is the number of adsorbed ions per unit area at $z = l$, and n'' is the number at $z = d - l$. The corresponding equation of state gives the surface pressure Π for all the ions together:

$$\Pi/kT = n' + n'' + B_{20}n'^2 + B_{11}n''n' + B_{20}n''^2 + B_{30}n'^3 + B_{21}n'^2n'' + B_{21}n'n''^2 + B_{30}n''^3 + \cdots \quad (4)$$

The second virial coefficients B_{20} and B_{11} may be interpreted approximately as indicating the area excluded to an ion by the presence of another ion on the same side (B_{20}) or the opposite side ($\frac{1}{2}B_{11}$). These coefficients may be calculated from the potential energy between a pair of ions using

$$B_{20} = \frac{1}{2}\int_0^\infty \{1 - \exp[-q\varphi(r, l)/kT]\}\, 2\pi r\, dr \quad (5)$$

and

$$B_{11} = \int_0^\infty \{1 - \exp[-q\varphi(r, d - l)/kT]\}\, 2\pi r\, dr. \quad (6)$$

The higher-order coefficients are given by integrals (Hirschfelder et al., 1954; Ree and Hoover, 1964) whose integrands are products of factors such as those in curly brackets in Eqs. 5 and 6.

The expression $\{1 - \exp[-q\varphi/kT]\}$ in Eq. 5 is almost equal to 1 whenever $q\varphi/kT > 3$. Hence, as noted before for the monolayer (Tsien, 1978), the virial coefficients and the electrochemical potential are insensitive even to gross

errors in the expressions used for φ whenever both they and the true φ yield large values.[2] The integrands $r[1 - \exp(-q\varphi/kT)]$ are plotted for burial depth $l = 0.2$ nm in Fig. 1 *b* as a function of ion separation r for the three different types of φ corresponding to same-side repulsion $[\varphi(r, l)]$, across-membrane repulsion $[\varphi(r, d - l)]$, and monolayers $[\varphi_m(r)]$. Numerical integration of the area under each of these curves yields the values of B_{20}, B_{11}, and B_{20}^m at $l = 0.2$ nm; repeating the calculations for other values of l yields Fig. 1 *c*.

In principle all the equilibrium properties of the adsorbed ions can be calculated from the infinite series for the electrochemical potential in Eq. 3 and the rules for calculating the virial coefficients B_{ij}. These equations are an exact statement of the mobile, discrete charge model. Unfortunately, the higher-order virial coefficients become rapidly more difficult to evaluate as i and j increase. Thus B_{30} requires a triple numerical integration over a product of three different factors each of the form $[1 - \exp(-q\varphi/kT)]$. This calculation is still manageable by direct summation of series and was confirmed for selected values of l by Monte Carlo methods. B_{30} ranges from 37 to 50% of B_{20}^2 as l increases from 0.025 to 0.4 nm. B_{30}^m was already known to be ~28% of $(B_{20}^m)^2$ (Tsien, 1978). However, our computing resources proved insufficient to evaluate B_{40}, the sum and difference of three five-dimensional infinite integrals of products of up to six of the usual factors. Because the positive and negative contributions are large but nearly cancelling, the net sum is particularly hard to obtain accurately.

Truncated Viral Approximation

At sufficiently low densities n, it should be possible to neglect the higher-order terms in Eqs. 3 and 4 whose virial coefficients have not been calculated. We call the resulting limiting law the truncated virial approximation.

The adsorption isotherm follows from Eq. 3 using $\Delta V = 0$, $n' = n'' \equiv n$, and an expression for the electrochemical potential of the dilute hydrophobic ions in the aqueous saline:

$$\mu'_{aq} = \mu''_{aq} = \mu^0_{aq} + kT \ln c = \mu' = \mu'' \qquad (7)$$

where c is the aqueous concentration. The result is

$$\beta c = n \exp[(2B_{20} + B_{11})n + \tfrac{3}{2} B_{30} n^2] \qquad (8)$$

where $\beta \equiv \exp[(\mu^0_{aq} - \mu^0)/kT]$ is the adsorption constant. For a monolayer, $2B_{20}^m$ replaces $2B_{20} + B_{11}$ in Eq. 8. Because for $l < 0.3$ nm, $2B_{20}^m \simeq 2B_{20} + B_{11}$ (see Fig. 1 *c*) and $B_{30}^m \simeq B_{30}$, the truncated virial approximation, like the smeared charge model (see Andersen et al., 1978), predicts that the adsorption isotherm to a symmetrical membrane when $n' = n''$ will be the same as to a monolayer. This approximate equality is the true justification of the then insufficiently supported assertion (Tsien, 1978) that the far side of a bilayer can be neglected in calculations of such isotherms.

The densities of ions adsorbed to monolayers and bilayers are usually not measured directly but can be related respectively to the compensation potential and to the amount of charge that can be transferred across the membrane. The relation between compensation (or surface) potential and concentration of adsorbed ions is the same (Grahame, 1958) whether the ions are treated as being discrete or smeared:

$$\Delta V_c = qnl/\epsilon\epsilon_0 . \qquad (9)$$

When an electric field is applied across a membrane, hydrophobic ions such as tetraphenylborate move rapidly between the two adsorption layers, but the total density of adsorbed ions, $n' + n'' = 2n$, varies very much more slowly, so that on the time scale of the experiment it can be considered constant. As a consequence of this redistribution between layers at l and $d - l$, the external circuit must move a charge

$$\Delta Q = q(d - 2l)(n' - n)/d \qquad (10)$$

from one surface to another if constant applied potential is to be maintained (see Andersen et al., 1978; Hladky and Tsien, 1979). The charge transfer that would be seen in the external circuit if all the ions could be shifted to one side is thus

$$\Delta Q_{max} = |q|(d - 2l)n/d . \qquad (11)$$

For finite applied potentials ΔV, the charge transfer ΔQ is given by the condition that the redistributed ions are again effectively at equilibrium between the two adsorption layers, i.e., $\mu' = \mu''$. From Eq. 3a and b, the potential ΔV necessary to achieve a given degree of ion transfer is given by

$$q\Delta V(d - 2l)/(kTd) = \ln (n'/n'') + (2B_{20} - B_{11})(n' - n'') + \tfrac{3}{2}B_{30}(n'^2 - n''^2) . \qquad (12)$$

[2]For lipid membranes and hydrophobic ions the electrostatic potential energy is already large before the ions can approach each other sufficiently closely for the short range interactions between them to have effect. Thus B_{20} is determined by the electrostatic repulsion and it is large. In contrast to the earlier treatment by Buff and Stillinger (1963) of the much thinner ($d \simeq 0.3$ nm) compact region of the double-layer, where B_{20} is small, here the Coulombic contribution to the integrand must not be linearized and no expression is required for the short range interactions (see also Levine et al., 1967). Similarly, because the experimental range of ion densities is well below complete coverage of the surface, here again in contrast to ions adsorbed at the mercury-water interface, it is not necessary to complicate Eq. 3 by including an expression to allow for the entropy of mixing of the ions with the lipid molecules (Levine et al., 1967).

Comparison of the Truncated Virial Approximation and Other Models with the Experimental Data

Does the truncated virial approximation fit the experimental data of Andersen et al. (1978)? As expected, only at low densities, as shown in Fig. 2, which tests the approximation on the adsorption isotherm to bilayers (Fig. 2 *a*), the compensation potentials ΔV_c on monolayers (Fig. 2 *b*), and charge redistribution as a function of transmembrane potential at one fairly high aqueous concentration (10^{-6} *M*) of tetraphenylborate (Fig. 2 *c*). Fig. 2 *a* shows that a burial depth l of 0.15 nm fits the adsorption isotherm up to 10^{-6} *M* but not beyond; Fig. 2 *b* shows that, though the low concentration data ($c \leq 3 \times 10^{-7}$ *M*) can be fitted by l = 0.2–0.25 nm, all the theoretical curves seriously overestimate the compensation potential ΔV_c at high concentrations. Because ΔV_c is directly proportional to surface charge density in a model-independent way (Eq. 9), the truncated virial approximation evidently lets too many charges adsorb at high aqueous concentrations. In other words, the approximation underestimates the true repulsion. The same conclusion may be drawn from Fig. 2 *c*; l = 0.4 nm is required to account for the large experimental reduction in the efficacy of applied potential at shifting charge.

Figs. 3 *a–c* analogously test the smeared charge model with which Andersen et al. (1978) interpreted their data for membranes. In the present formalism the smeared charge model is tantamount to setting B_{30}, B_{21}, etc. to zero in Eq. 3 and replacing $2B_{20}kT$ and $B_{11}kT$ by $q^2l(d-l)/(\epsilon\epsilon_0 d)$ and $q^2l^2/(\epsilon\epsilon_0 d)$, respectively. Fig. 3 *a* shows that the smeared charge model can also fit the adsorption isotherm up to 10^{-6}*M* but not beyond, though the burial depth that does it is only 0.025 nm, six times less than the burial depth that works best in the truncated virial model. The predicted compensation potentials are now completely wrong, even at the very lowest concentrations, as noted by Andersen et al. (1978), though the error is in the opposite direction, i.e., the model underestimates the true charge density or overestimates the repulsion. Fig. 3 *c* shows that the charge transfer curves can be fitted by l = 0.10 nm, but this value is incompatible with the l of 0.025 nm from Fig. 3 *a*.

Andersen et al. (1978) noted the complete inability of any smeared charge model to predict the observed monolayer compensation potentials, and therefore considered a hexagonal lattice model as an example of a discrete charge model. In this model, the electrostatic potential energy of the ions is calculated by assuming that the ions are fixed on a lattice so that each ion has six equidistant nearest neighbors. This arrangement gives the minimum potential energy for a given density of ions but demands complete order (or zero entropy). It is well recognized (see Barlow and MacDonald, 1967) that the lattice model is most

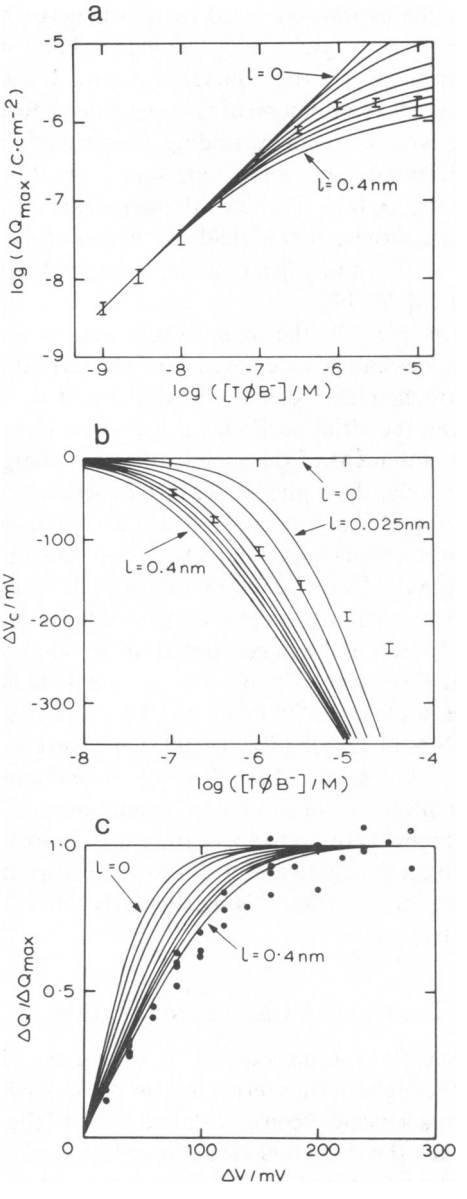

FIGURE 2 Comparison of the predictions of the truncated virial approximation with experimental data of Andersen et al., 1978. All the theoretical curves are calculated for ϵ = 2.1 and d = 3.51 nm. (*a*) Comparison of adsorption isotherms as assessed by maximum charge transfer ΔQ_{max} when a very large potential difference is suddenly imposed. ΔQ_{max} is related to n, the true density of adsorbed ions, by Eq. 1. The aqueous concentrations c of tetraphenylborate are denoted [TØB$^-$] with units of moles per liter. The smooth curves are the theoretical predictions for l = 0, 0.025, 0.05, 0.10, 0.15, 0.20, 0.25, 0.30, and 0.40 nm, respectively. The adsorption constant β was set to $[d/(d-2l)] \cdot 0.0432$ cm as dictated by the low-concentration experimental points. (*b*) Comparison of predicted and observed compensation potentials ΔV_c on a monolayer, as functions of c. The l and β values are the same as in (*a*). (*c*) Comparison of predicted and observed charge transfers, normalized to ΔQ_{max}, as a function of applied membrane potential ΔV, for $c = 10^{-6}$ M. This value of c was chosen because it was the highest for which experimental data were presented in Andersen et al., 1978, and shows the effects of charge interaction most prominently.

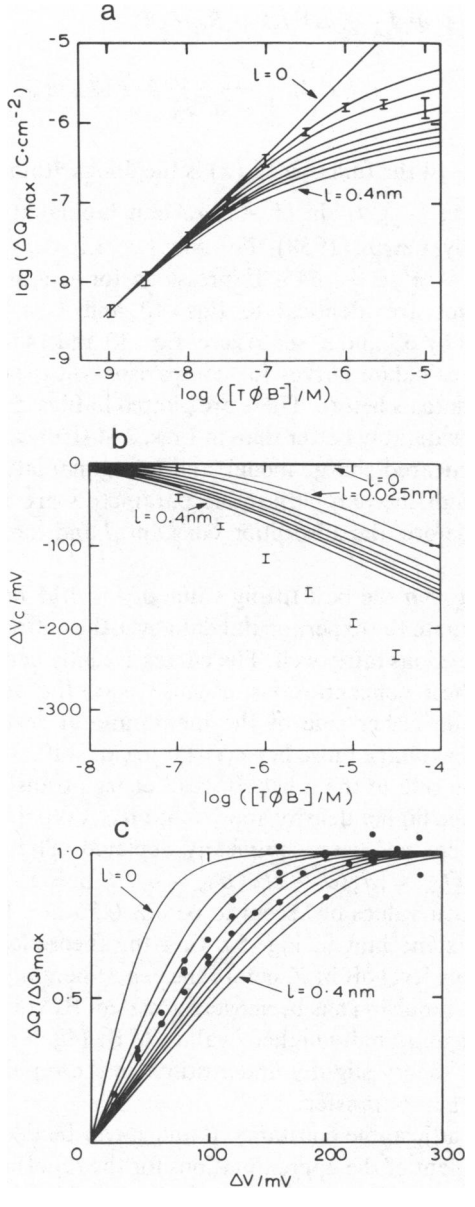

FIGURE 3 Comparison of the predictions of the smeared charge model with the same experimental data as in Fig. 2. The same values of ϵ, d, l, and β were assumed. (*a*) Adsorption isotherm; (*b*) compensation potentials; (*c*) charge transfer curves.

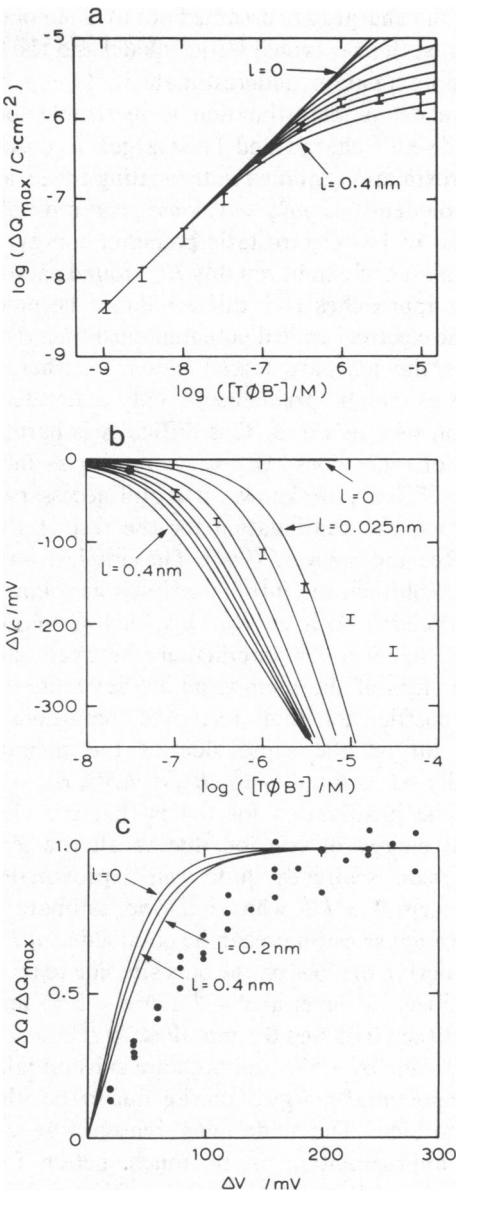

FIGURE 4 Comparisons of the predictions of the hexagonal lattice model with the same experimental data as in Fig. 2. The same values of ϵ, d, and β $(d - 2l)/d$ were assumed, and the same values of l have been used in parts *a* and *b*. (*a*) Adsorption isotherms; (*b*) compensation potentials; (*c*) charge transfer curves for l = 0, 0.2 and 0.4 nm. In part (*c*) note that the curve for 0.4 nm is to the left of the curves for 0 and 0.2 nm. Other values of l are omitted for clarity because they closely overlap the values shown.

realistic at high densities and low temperatures, and becomes poorer when the ions have room and kinetic energy to wander. How good is it under the present experimental conditions? The predictions of this model are derived in the Appendix and graphed in Fig. 4 *a–c*. The predicted compensation potentials are somewhat steeper than those from the truncated virial approximation, which were already too steep. Finally, the charge-transfer curves are even further to the left than for the truncated virial approximation.

For completeness, yet another discrete charge model, the "cut-off disk" model, is also discussed in the Appendix. Because this is yet another model that gives weaker repulsions than the truncated virial approximation, detailed figures are not presented.

An Approximate Continuation of the Virial Expansion Power Series

Evidently the smeared charge model overestimates the effect of electrostatic repulsion, which is to be expected

because the charges are assumed not to avoid one another. By contrast the hexagonal lattice model and the truncated virial approximation underestimate it. In the hexagonal lattice model, underestimation is inevitable, but in the mobile, discrete charge model it is largely a consequence of the approximation entailed in truncating the series. At low adsorption densities, $nB_{20} \ll 1$, ions spend most of the time in regions of low electrostatic potential energy, i.e., each avoids an area of extent roughly B_{20} around each other ion. When n approaches B_{20}^{-1}, this avoidance becomes impossible. The electrochemical potential must then rise dramatically as the ions are forced closer together. Such an increase cannot be predicted by only a few terms of an expansion such as Eq. 3. This difficulty is hardly new. In theories of other dense gases, even when as many as six virial coefficients are known, it is still necessary to devise an approximate continuation for the rest of the infinite series (Ree and Hoover, 1964). The simplest way we have found to continue the infinite series is as follows: (*a*) All the coefficients such as B_{21}, B_{22}, or B_{31} in Eq. 3 that describe higher-order interactions between charges on opposite sides of the membrane are set to zero. (*b*) The higher coefficients that relate to repulsions between charges all on the same side of the membrane are arbitrarily set as $B_{30} = \frac{1}{2}B_{20}^2$, $B_{40} = \frac{1}{3}B_{20}^3$, $B_{50} = \frac{1}{4}B_{20}^4$ and so on. The justification for (*a*) is that the electrostatic potential energy of one ion due to all the ions on the opposite side is already quite well approximated by the existing term $B_{11}n''kT$, which is a lower estimate of the true value. An upper estimate can be obtained as $q^2l^2n''/(\epsilon\epsilon_0 d)$ by considering the ions on the opposite side to be uniformly smeared over the layer at $d - l$. For $d = 3.51$ nm, $\epsilon = 2.1$, and l between 0.05 and 0.3 nm, these bracketing estimates differ in value by <5%, and both are substantially smaller than the potential energy of one ion due to the other ions on the same side. The underlying reason why a smeared charge approximation is so much better for across-membrane repulsions than for same-side repulsions is that the former are much weaker. Fig. 1 shows that the repulsion energy for a pair of ions on opposite sides of the membrane remains much less than kT even at closest approach; therefore from the point of view of the ion whose energy we are considering, the ions on the far side are hardly perturbed from a uniform random distribution.

Assumption (*b*) is adopted because it is simple, gives mathematically compact expressions, gets B_{30} approximately correct, and gives the desired steep rise in repulsion as n approaches B_{20}^{-1}. Thus the surface pressure and chemical potentials become

$$\frac{\Pi}{kT} = n'[1 - \ln(1 - n'B_{20})] + n''[1 - \ln(1 - n''B_{20})] + B_{11}n'n'', \quad (13)$$

$$\mu' = \mu^0 + ql\Delta V/d + B_{11}n''kT + kT\left[\ln\frac{n'}{1 - n'B_{20}} + \mathrm{Li}_2(n'B_{20})\right] \quad (14a)$$

$$\mu'' = \mu^0 + q(d - l)\Delta V/d + B_{11}n'kT + kT\left[\ln\frac{n''}{1 - n''B_{20}} + \mathrm{Li}_2(n''B_{20})\right]. \quad (14b)$$

In Eq. 14 the function $\mathrm{Li}_2(x)$ is the dilogarithm function defined as $-\int_0^x t^{-1}\ln(1 - t)\,dt$ and tabulated and discussed by Lewin (1958). For small x, $\mathrm{Li}_2(x) \simeq x$, and $\mathrm{Li}_2(1) = \pi^2/6 \simeq 1.645$. Expressions for μ and Π on a monolayer are identical to Eqs. 13 and 14 a with B_{20} replaced by B_{20}^m and n'' set to zero. Eqs. 13 and 14 have been used to calculate curves for comparison with the experimental data as before. These are plotted in Figs. 5 *a–c*. The fit is considerably better than in Figs. 2–4 (truncated virial series, smeared charge model, and hexagonal lattice model), though the only adjustable parameters are the same two as before, the adsorption constant β and the depth of burial l.

In Fig. 5 *a* the best-fitting value of l is 0.15 nm, which can simulate the experimental data over the entire range of concentrations fairly well. The curves actually bend over at the highest concentrations because once the adsorption density on either side of the membrane at rest exceeds $\frac{1}{2}B_{20}^{-1}$, no voltage pulse however large can shift all the ions from one side to the other. Instead charge transfer has to stop as the higher density approaches B_{20}^{-1}, even if the lower density has not been completely depleted. Thus for $n > \frac{1}{2}B_{20}^{-1}$, $\Delta Q_{max} = |q|(d - 2l)(B_{20}^{-1} - n)/d$. In Figs. 5 *b* and *c* the best-fit values of l seem to be 0.2–0.25 nm. However, there is some hint in Fig. 5 *b* that the theoretical curves ultimately level off in V_c before the experimental points do, i.e., that repulsion has been overestimated. By contrast, the need for marginally higher l values to fit Fig. 5 *c* suggests that the theory slightly underestimates the repulsion hindering charge transfer.

Both adjustable constants, β and l, can be determined, independent of the approximations for the repulsion terms, from the data for very low tetraphenylborate concentrations (10^{-9} to 10^{-8} M) where the adsorbed charges are so sparse that they interact negligibly with each other. In that domain the fraction of the total membrane potential acting between the adsorption planes, $(d - 2l)/d$, can be determined from precise measurements of charge transfer ΔQ as a function of membrane potential ΔV, as may be seen from Eq. 12 by neglecting the repulsion terms. Andersen (1978) thereby estimated $(d - 2l)/d$ as 0.85 to 0.90, corresponding to $l = 0.18$ to 0.26 nm. This independent estimate confirms the reasonableness of the range $l = 0.15$–0.25 nm derived from Figs 5 *a–c*. As for the adsorption constant β, the observed ratio of ΔQ_{max} to c for $c \leq 10^{-8}$M dictates that $\beta(d - 2l)/d$ must equal ~0.04 cm for all of the approximations considered. Thus there is very little room to vary β in fitting the high concentration data.

Probably the most severe deficiency of the mobile discrete charge model is the difficulty of directly calculating B_{40}, B_{50}, ..., to confirm the estimates of their

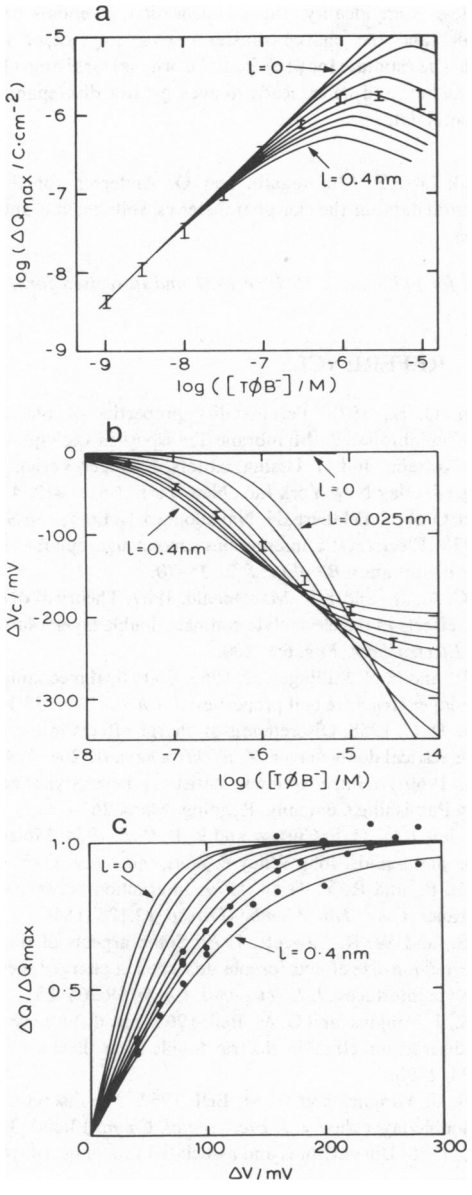

FIGURE 5 Comparison of the predictions of the extended virial expansion (Eq. 14) with the same experimental data as in Figs. 2–4. The same values of ϵ, d, l, and β were assumed. (*a*) Charge transferred on application of a large voltage, as a function of aqueous tetraphenylborate concentration; (*b*) compensation potentials; (*c*) charge transfer curves at 10^{-6} M as a function of applied potential. In (*a*) the large voltage was 200 mV; on the scale of this graph, the only visible effect of assuming a voltage of 300 mV or greater is to sharpen the peak of each curve.

magnitude. Fortunately the qualitative behavior of the predicted curves is much the same for a range of alternative ways of extending the power series. Thus if B_{30}, B_{40}, B_{50} . . . are set to B_{20}^2, B_{20}^3, B_{20}^4 . . . then the repulsions for any given l are strengthened, so that l values from 0.1 to 0.2 nm are the best fitting. Alternatively, if B_{30}, B_{40}, B_{50} . . . are taken as $\frac{1}{2}B_{20}^2$, $\frac{1}{4}B_{20}^3$, $\frac{1}{8}B_{20}^4$, etc., the repulsions prove somewhat weaker than in Eqs. 13 and 14, so l = 0.2 to 0.3 nm becomes the preferred range. We know that B_{30} correctly calculated from the model is somewhat $< \frac{1}{2}B_{20}^2$; if the exact B_{40}, B_{50}, etc., were also markedly below the assumed values which give good fits in Fig. 5*a–c*, that would indicate that the mobile discrete charge model omits physical interactions that contribute to repulsion specifically at the highest densities. Such interactions might include direct steric interferences from the nonzero volumes of the ions, or dielectric saturation, or partial failure of the assumed isopotentiality of the aqueous saline-lipid interface. Nevertheless, the mobile discrete charge model makes fewer unrealistic physical assumptions then any of the previous models. It is also better than the others at fitting all three types of experiment at once, even when its virial expansion is severely truncated (Fig. 2 *a–c*). With a plausible continuation for its infinite series (Eqs. 13 and 14) it does remarkably well at explaining almost all the experimental data with a narrow range of its most important free parameter, the depth of burial l, closely matching estimates from independent experiments. This success indicates the utility of explicitly considering lipid-soluble ions in membranes as discrete charges whose lateral distribution is controlled by equilibrium statistics.

APPENDIX

In the conventional hexagonal lattice and cut-off disk models, adsorption isotherms for ions are calculated from a micropotential and the Boltzmann equation, sometimes with an additional factor to account for the entropy of mixing of the ions with the other molecules adsorbed at the surface. The micropotential in turn is the electrostatic potential at the site of one ion which results from the presence of all the other ions. It is calculated from a pair potential (e.g., Eqs. 1 or 2) and an assumed distribution of the other adsorbed ions. The approximations inherent in these procedures have been reviewed (MacDonald and Barlow, 1964; Barlow and MacDonald, 1967; Levine et al., 1967).

Hexagonal Lattice Model

If the ions are assumed to be hexagonally close packed, i.e., adsorbed to the vertices of a triangular lattice, the spacing between nearest neighbours, $s(n)$, is related to the surface density n by $s(n) = 2^{1/2}\,3^{-1/4}\,n^{-1/2}$. The contribution to the micropotential from ions on the same side of the membrane becomes

$$\psi(n) = \sum_{\text{lattice}} \varphi(r, l) = 6 \sum_{i=1}^{\infty} \sum_{j=0}^{i-1} \varphi[(i^2 - ij + j^2)^{1/2}\, s(n), l] \quad \text{(A1)}$$

where $\varphi(r, l)$ is the pair potential given by Eq. 2 with $z = l$. The potential due to ions on the opposite side depends upon the registration of the two lattices. In positive registration the closest ion on the opposite side is assumed to be directly opposite, but in negative registration the closest ion is as far away as allowed by the lattice spacing. Positive registration is not preferred. There are, however, two difficulties that prevent immediate acceptance of negative registration. First, even if same side repulsion is strong enough to impose a local lattice structure, opposite side repulsions will not be strong enough to impose negative registration, as argued in the main text. Second, negative registration cannot be maintained for all ions at once unless the surface densities and lattice spacings on the two sides are identical. There can be little doubt that the opposite side contribution should lie somewhere between the two registrations, and that at low densities a more accurate estimate than either of the extremes can be obtained by assuming that opposite side ions are smeared. Fortunately, at high densities the estimates from the two registrations converge to the same value as the smeared charge estimate. For instance even for very

deep burial that overstates opposite side repulsion, $l = d/2\pi$, and for a charge density near the upper end of the experimental range so that $s(n) = d = 3.51$ nm the positive and negative registration estimates differ from the smeared charge estimate, $2.88kT/q$, by only $0.26kT/q$ and $-0.17\ kT/q$ respectively. Therefore in our calculations we have used the smeared charge estimate, $n''ql^2/(\epsilon\epsilon_0 d)$, for the part of the micropotential contributed by the ions on the far side of the membrane. Thus the chemical potentials of the ions on the two sides of the bilayer are given by

$$\mu' = \mu^0 + kT \ln n' + ql\Delta V/d + q\psi(n') + q^2l^2n''/(\epsilon\epsilon_0 d) \quad \text{(A2)}$$

$$\mu'' = \mu^0 + kT \ln n'' + q(d - l)\Delta V/d + q\psi(n'') + q^2l^2n'/(\epsilon\epsilon_0 d). \quad \text{(A3)}$$

On a monolayer the lattice sum analogous to (A1) is known (Andersen et al., 1978) to yield $8.89\ ql^2n^{3/2}/(2\pi\epsilon\epsilon_0)$, so that

$$\mu_m = \mu^0 + kT \ln n + 8.89\ q^2l^2\ n^{3/2}/(2\pi\epsilon\epsilon_0). \quad \text{(A4)}$$

Figures 4*a–c* were calculated from Eqs. (A2) – (A4) in close analogy to Eqs. 7–12.

Andersen et al. found that the hexagonal lattice model produced an excellent fit of just the monolayer compensation potential data if ϵ as well as l was allowed to vary. However, the best fit values of l and ϵ were 1.0 nm and 8 respectively; unfortunately this value of l is much too large to fit the membrane data, and $\epsilon = 8$ is unrealistically large for a monolayer which was assumed to have a uniform dielectric constant throughout its thickness.

Cut-off Disk Model

In the cut-off disk model, an ion is surrounded by a circular charge free region. Beyond the cut-off radius, the charge is taken as smeared at constant density. Grahame (1958) proposed that the area of the disk should be the same as the area per adsorbed ion. Levine et al. (1965; 1967; for more recent references see Levine and Fawcett, 1979) have shown that the area per ion is much too large as an estimate for the area of the disk at low ion densities, and have suggested instead a revised cut-off disk model. For low ion densities, they propose a constant cut-off radius r_{co} defined by

$$\pi r_{co}^2 = \int_0^\infty [1 - \exp(-q\varphi/kT)]2\pi r\, dr = 2B_{20}. \quad \text{(A5)}$$

They then calculate the same-side contribution to the micropotential as

$$\psi(n) = n \int_{r_{co}}^\infty \varphi(r)2\pi r\, dr. \quad \text{(A6)}$$

Wang and Bruner (1978) have used a similar model to treat the non-equilibrium properties of ions adsorbed to membranes.

In the Levine et al. revised cut-off model, $\psi(n)$ is proportional to n, so that the predictions of the model using Eqs. A2 and A3 have the same functional form as a virial expansion truncated after the B_{20} and B_{11} terms. However, because $q\psi(n) < 2B_{20}nkT$ for each l, the revised cut-off model predicts yet weaker repulsions, i.e., the predicted adsorptions deviate less from ideality, the compensation potentials are larger in magnitude, and the charge-transfer curves are steeper functions of potential. The estimate for $\psi(n)$ from the original Grahame (1958) model is even smaller, and hence leads to even greater discrepancies with the experimental data.

We thank Drs. S. McLaughlin and O. Andersen for the tabulated experimental data for the charge transfer vs. voltage plots and for helpful discussion.

Received for publication 16 June 1981 and in revised form 15 January 1982.

REFERENCES

Andersen, O. S., 1978. Permeability properties of unmodified lipid bilayer membranes. *In* Membrane Transport in Biology. G. Giebisch, D. C. Tosteson, and H. Ussing, editors. Springer-Verlag, Berlin, and Springer-Verlag New York Inc., New York. 1:411–412, 434–444.

Andersen, O. S., S. Feldberg, H. Nakadomari, S. Levy, and S. McLaughlin. 1978. Electrostatic interactions among hydrophobic ions in lipid bilayer membranes. *Biophys. J.* 21:35–70.

Barlow, C. A., Jr., and J. R. MacDonald, 1967. Theory of discreteness of charge effects in the electrolyte compact double layer. *Advan. Electrochem. Electrochem. Eng.* 6:1–200.

Buff, F. P., and F. H. Stillinger, Jr. 1963. Statistical mechanical theory of double-layer structure and properties. *J. Chem. Phys.* 39:1911–1923.

Grahame, D. C. 1958. Discreteness-of-charge effects in the inner region of the electrical double layer. *Z. Elektrochem.* 62:264–274.

Hill, T. L. 1960. An introduction to statistical thermodynamics. Addison-Wesley Publishing Company, Reading, Mass. 261–275.

Hirschfelder, J. O., C. F. Curtiss, and R. B. Bird. 1954. Molecular theory of gases and liquids. John Wiley & Sons, Inc., New York. 131–233.

Hladky, S. B., and R. Y. Tsien. 1979. Interaction between ions in lipid membranes. *Curr. Top. Membr. Transp.* 12:126–164.

Levine, S., and W. R. Fawcett. 1979. Some aspects of discreteness of charge and ion-size effects for ions adsorbed at charged metal/aqueous electrolyte interfaces. *J. Electroanal. Chem.* 99:265–281.

Levine, S., J. Mingins, and G. M. Bell. 1965. The diffuse layer correction to the discrete ion effect in electric double layer theory. *Can. J. Chem.* 43:2834–2866.

Levine, S., J. Mingins, and G. M. Bell. 1967. The discrete-ion effect in ionic double-layer theory. *J. Electroanal. Chem.* 13:280–329.

Lewin, L. 1958. Dilogarithms and associated functions. Macdonald Ltd., London.

MacDonald, J. R., and C. A. Barlow, Jr. 1965. In the Proceedings of the First Australian Conference on Electrochemistry. J. A. Friend and F. Gutmann, editors. Pergamon Press Ltd., Oxford.

McLaughlin, S. 1977. Electrostatic potentials at membrane-solution interfaces. *Curr. Top. Membr. Transp.* 9:71–144.

Ree, F. H., and W. G. Hoover. 1964. Fifth and sixth virial coefficients for hard spheres and hard disks. *J. Chem. Phys.* 40:939–950.

Tsien, R. Y. 1978. A virial expansion for discrete charges buried in a membrane. *Biophys. J.* 24:561–567.

Wang, C.-C., and L. J. Bruner. 1978. Evidence for a discrete charge effect within lipid bilayer membranes. *Biophys. J.* 24:749–764.